SoLID pre-R&D
Second Quarterly Progress Report

December 2020 to March 2021

SoLID Collaboration

April 16, 2021

Contents

1 DAQ

1.1 Summary

This chapter summarizes the SoLID DAQ pre-R&D activities for the third quarter, from December, 2020 to March, 2021.

The five main on-going tasks (A-E) for this pre-R&D report are:

- A) GEM VMM3 readout high rate testing to determine trigger rate capability, behavior with pile-up, and readout performance
- B) GEM APV25 readout high rate testing: show that 100 kHz trigger rate is achievable with existing readout hardware developed for SuperBigBite (SBS)
- C) FADC developments for fast readout and triggering
- D) Beam test of gas Cherenkov readout with analog sums and MAROC chip
- E) Time of flight using the NALU sampling chip

A - VMM development is making good progress with the first readout of the digital path from the evaluation board. Design of the prototype board is well advanced some delay due to chip availability.

B - Rate measurements with the APV25 show a capability of 100 kHz for the current estimated occupancy for the SoLID SIDIS configuration. Several readout firmware improvements were implemented.

C - The fast FADC VXS readout was completed in March. (It had been delayed in order to devote manpower to the Cerenkov beam test while beam was available.) Additional work on the DAQ software is on-going to support this feature.

D - A test bench for testing the MAROC along with FADC readout was setup. Data with LED and laser were taken. Testing with cosmic rays is on-going.

E - A spare sampling chip was received in November. Data with a pulser were acquired in December. Data from a single detector were recorded in January. A Test stand is being assembled for final measurement of timing resolution cosmic rays.

1.2 Milestones

1.2.1 GEM testing milestones

A) VMM3 We are studying the behavior of the VMM3 with high background and are determining the maximum trigger rate that can be achieved.

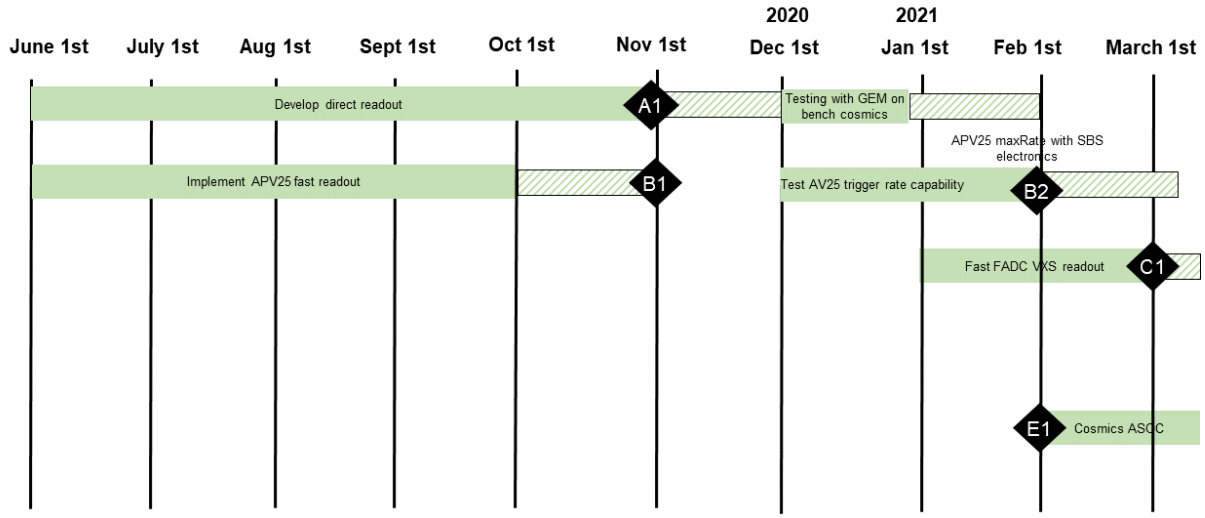

Figure 1: SoLID Pre-R&D for DAQ timeline, June 2020-March 2021

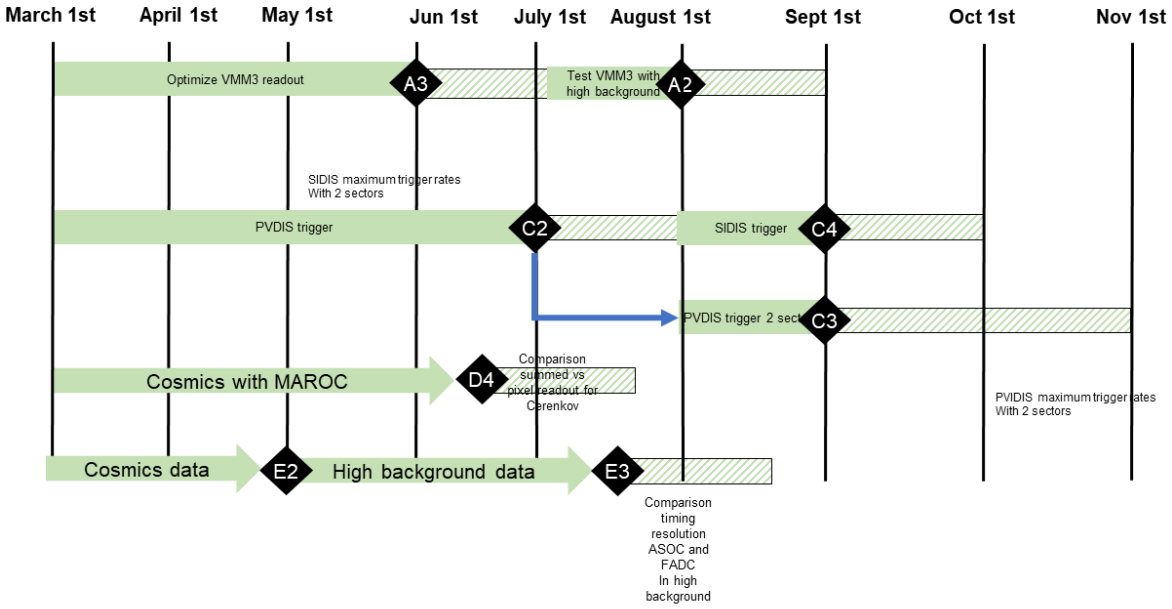

Figure 2: SoLID Pre-R&D for DAQ timeline, March 2020-November 2021 (hashed boxes are for the float)

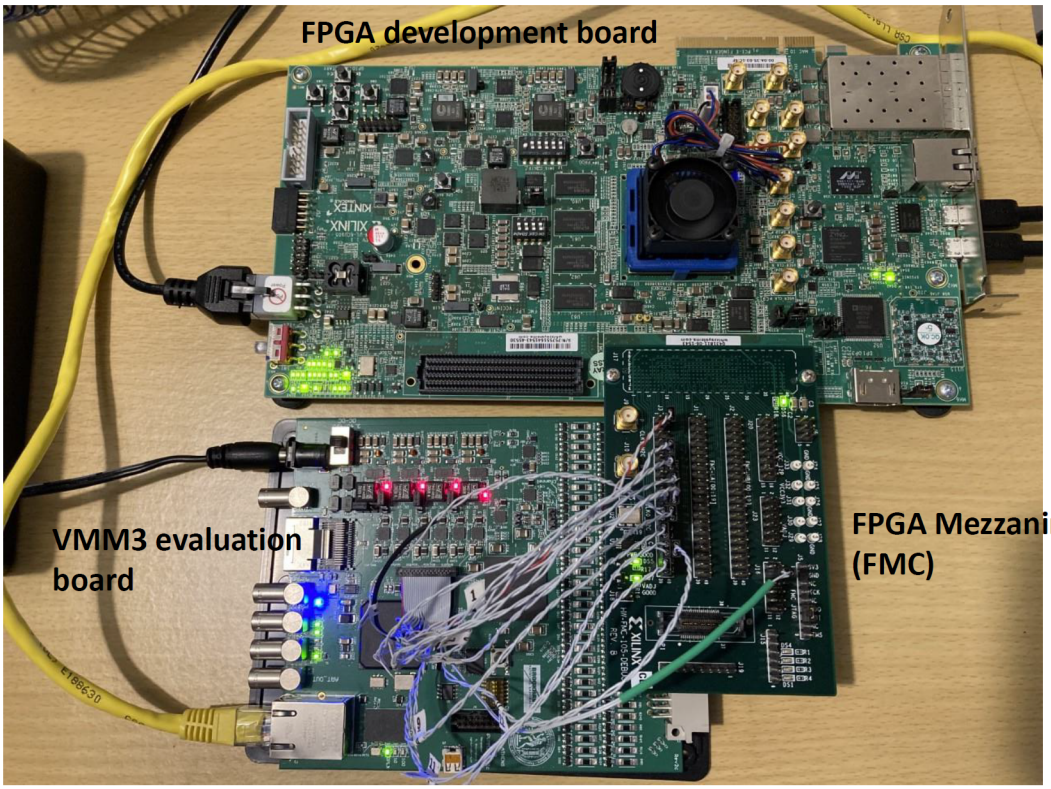

Figure 3: VMM evaluation board and FPGA development board

Milestone	Objectives	Expected Completion Date	Status	Updated Date
A1	Finish development of VMM3 direct readout	May 1, 2020	Complete	
A2	High rate testing with detector	July 15 2021	80% complete	August 1, 2021 +1 mo. conting.
A3	Optimized VMM3 setup for maximum data rate	May 15, 2021	70% complete	June 1, 2021 +1 mo. conting.

A2: VMM3 evaluation board system – The GPVMM evaluation board drives 6-bit ADC direct data from 12 channels out on a connector. This connector is cabled to a Xilinx FPGA development board for readout of the data.

Firmware for decoding the VMM direct output data and formatting it for readout was developed and simulated. We have successfully read out the direct output data via 1 Gb Ethernet. Figure 4 shows the distribution of ADC values for a single channel that is excited

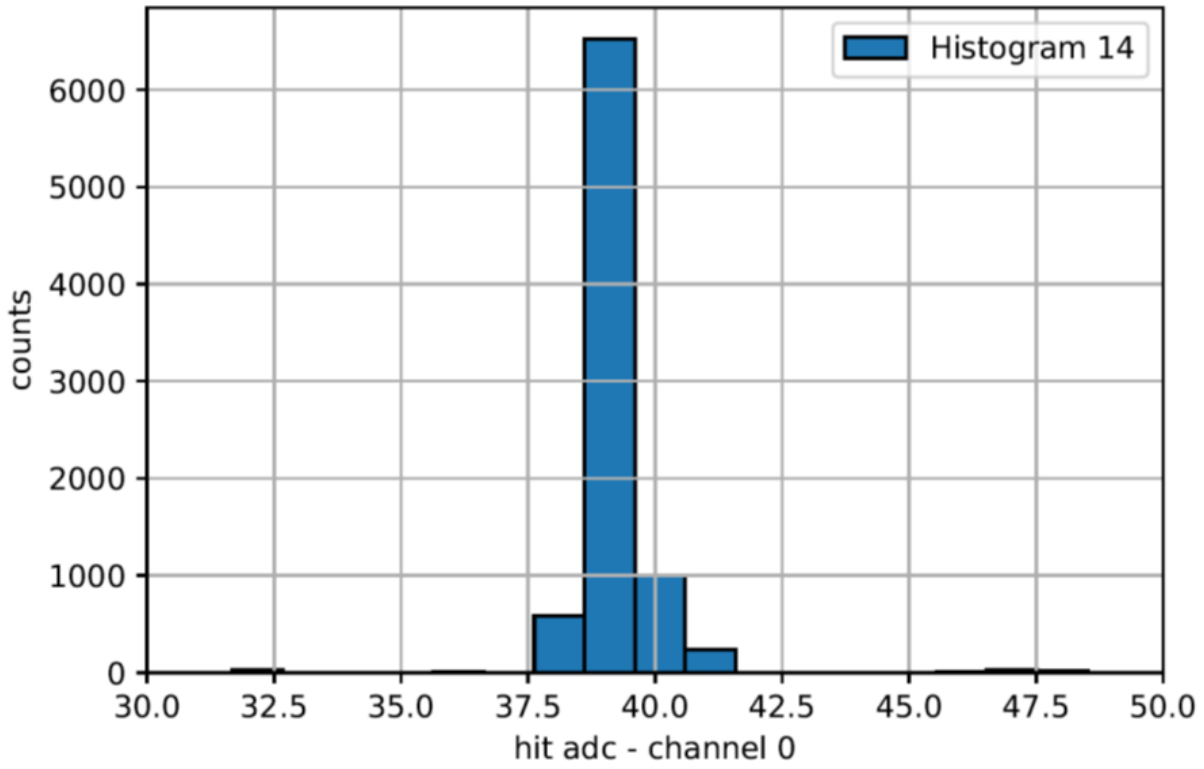

Figure 4: VMM 6-bit ADC direct data distribution from evaluation board

by test pulses generated in the VMM chip. The mean 6-bit ADC value of 39 is consistent with the mean 10-bit ADC value of 620 read out through the VMM chip's normal readout path.

The evaluation board was tested with a 10 cm x 10 cm GEM with cosmics, but the small area covered made (1/20th of the GEM) it difficult to detect cosmics. A new test setup with a radioactive source is being assembled in area of the lab designated for radioactive source use. The final measurement will be done with the prototype board which will have more channels thus reducing the required time for cosmic ray data taking.

A3: Prototype front-end board – We are developing a prototype board that supports 128 VMM3 channels and mounts on a GEM detector with a high-pin count connector. It is designed with dual readout paths. The 10 GbE (Gigabit Ethernet) optical readout path allows for easy connection to a PC or network switch and is suitable for test stands or use in low radiation environments. The second path, the GBT (GigaBit Transceiver) optical readout link uses rad hard components designed for CERN LHC experiments and would be used for the SoLID experiment data readout. The module has a hit rate capability of several MHz per channel at a 200 KHz trigger rate which exceeds the requirements of SoLID. The printed circuit board design (layout, signal routing) is approximately 85% complete.

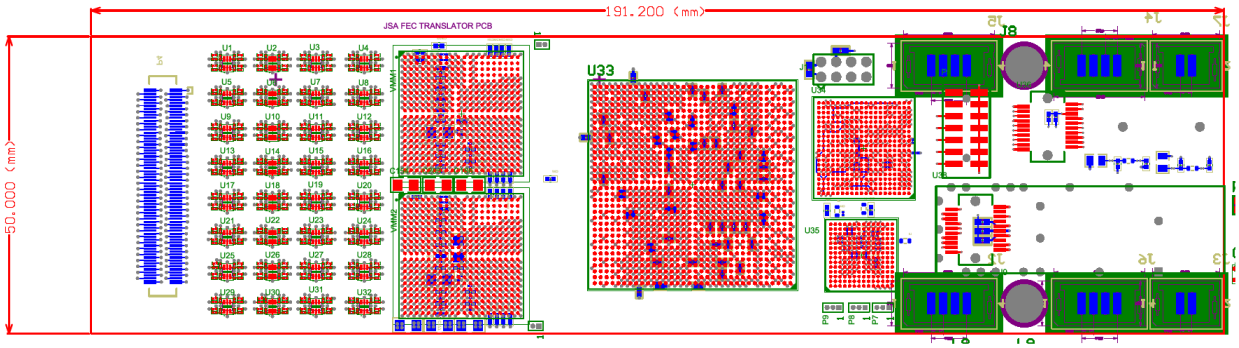

Figure 5: VMM prototype board layout

Firmware developed for the VMM evaluation board system described in Fig. 3 has been scaled up to 128 channels and simulated.

The design was implemented in the target FPGA (Xilinx XCKU035) and uses about 20% of the device's resources. This should allow ample headroom for us to implement the Triple Modular Redundancy (TMR) techniques necessary to mitigate against logic upsets due to radiation exposure. We are expecting to receive the VMM3 chips required for the prototype board by April 25, 2021.

B) APV25 To test the feasibility of reusing electronics from SBS to reduce electronics costs, we will determine if the existing APV25 based electronics can reach a trigger rate of at least 100 kHz.

- Milestone B1, June 1, 2020: While the intrinsic specs of the chip should allow a 200 kHz trigger rate using one sample, some development is needed to determine if this is achievable with the existing SBS electronics. The task involves enabling APV25 buffering and optimizing the data transfer of the readout.

- Milestone B2, October 1, 2020: Determine rate limits of the APV25 trigger and test in a high occupancy environment.

o Milestone	Objectives	Expected Completion Date	Status
B1	Finish development of fast APV25 readout	November 1, 2020	Complete
B2	Determine maximum rate achievable with APV25	March 15, 2021	Complete

B1: Completed in the second quarter.

B2: With the latest code using an MPD & SSP with 15APVs, the trigger rate is limited to about 5kHz with 6 samples at 100% occupancy. This corresponds to 100 kHz with 12 APVs with 1 sample at 30% occupancy. Higher rates are achievable by reducing the number of APV per board. An upgraded version of the APV readout board would allow to double the rate.

1.2.2 DAQ test stand and rate tests

C) DAQ

Milestone	Objectives	Expected Completion Date	Status	Updated Date
C1	Development of FADC readout through VXS	November 1, 2020	Complete	
C2	Testing PVDIS trigger functionalities and rate capability	May 1, 2021	50% complete	July 1, 2021 +1 mo. conting.
C3	PVDIS trigger test with two sectors	July 15, 2021	Started	September 1, 2021 +2 mo. conting.
C4	Test SIDIS trigger	August 15, 2021	Not Started	September 1, 2021 +1 mo. conting.

C1: Firmware and simulations are completed. The firmware has been compiled for the targets (VTP and FADC) utilizing a small fraction of available resources. Thus there is no concern about future changes overloading the resources of these boards. A simulation of a full crate of FADCs with full occupancy was performed. This showed that saturation of the 10GbE interface is achievable (in practice a 900MB/s limit is expected). The simulation produced a file in the the JLab EVIO format that can be read using standard JLab EVIO display tools (e.g. jeviodmp).

C2: Testing of the PVDIS trigger functionality and rates is on-going. The dead time of FADC in raw mode has been measured. Input signals are simulated using the FADC playback feature. A pulse with a 44 ns width and 10 ns rising time, which is similar to expected alorimeter signals, was defined for 15 channels and saved in the FADC RAM. The FADC loads the simulated pulses and injects them into processing pipeline for each trigger generated by the random pulser. The VTP collects the FADC data and generates the trigger based on the signal from the channels as shown in Fig. 6.

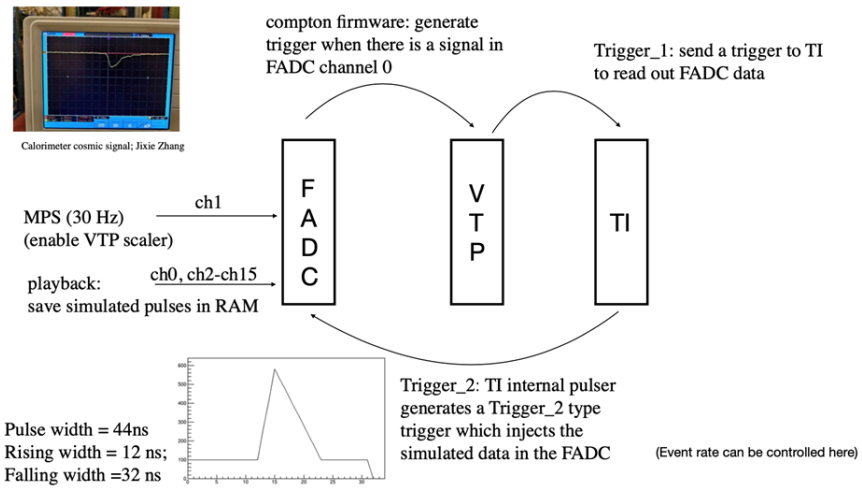

Figure 6: UMass Test setup for deadtime measurement

The FADC runs in raw mode, where every 4 ns the sample of the signal is recorded. The dead time measurements are performed by changing the rate of the TI internal pulser and made with two different readout window size: 128 ns and 192 ns. The results are shown in Fig. 7. At 20 kHz (maximum reate in one PVDIS sector), the FADC dead time is about 1%. This is before the FADC fast readout was implemented, so we expect that the FADC dead time will be much smaller than 1%. The dead time measurement will be performed again once the FADC fast readout is ready to use with CODA.

While the engineers are developing the FADC fast readout, work continues on the VTP FPGA design to find clusters in the calorimeter and to generate triggers from the clusters. This work is performed under the guidance of JLab FPGA experts. First, a map between the FADC channels and the block geometry is built. Every 32 ns when FADC reports the hits, the VTP filters out the hits that pass an energy threshold so that they can be treated as the "candidate" as the center of a cluster. Then for each of the candidate hit, it checks if the surrounding six blocks have hits within 16 ns, while the candidate hit (central block) still has the maximum energy deposit. If more than one surrounding block has a hit that meet the requirements, a cluster is formed. This algorithm is written in C and tested in the "vivado_hls" C simulation, where a "main" function generates random hits for 147 FADC channels. Currently, we are working on the optimization of the C code to get a good synthesis of the C code that will have the correct clock cycle and small latency.

We plan to generate a small asymmetry similar to expected signal (about 700 ppm) at a rate of about 20 kHz with a 120 Hz helicity flip, and see how accurately the FADC is able to measure this asymmetry. A combination of a Voltage-to-Frequency (VtoF) module and a helicity timing board, which can generate voltages at mV step, will be able to generate the desired small asymmetry. We have purchased and collected the modules that are needed for

the test which will be performed soon.

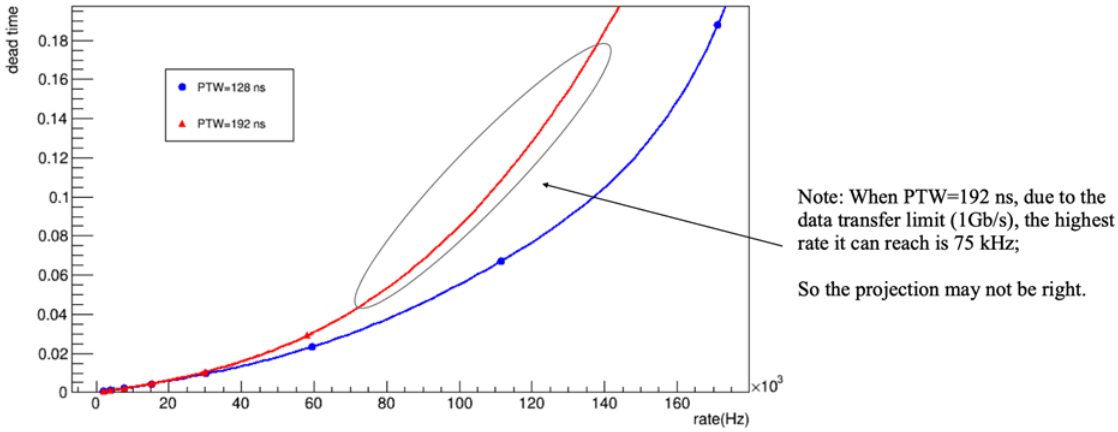

Figure 7: Deadtime measured as a function of trigger rate

C3: Start gathering/ordering equipment for test, requires C1 to be completed before data transfer between several crates can be implemented.

C4: Testing of the SIDIS trigger will start after electron trigger is finished

D) Cherenkov readout

Milestone	Objectives	Expected Completion Date	Status	Updated Date
D1	Setup FADC crate for Cherenkov simple sum testing	February 15, 2020	Complete	
D2	Record beam data using simple sum and FADC	September 15, 2020	Complete	
D3	Record data using MAROC sum readout	Oct 15, 2020	70% complete	June 15, 2021 +1 mo. conting.

D1: Completed in first quarter.

D2: Completed in second quarter.

D3: The MAROC sum electronics were delivered from INFN and are ready for a beam test. Due to a lack of available beam time, the beam test of the MAROC sum electronics was cancelled. We are continuing bench testing using LED, laser, and cosmic rays. We finished the laser and LED test this quarter and the cosmic ray test is ongoing. The details are in the Cherenkov section 2.5.

E) Time of flight The current baseline readout of the TOF is based on the FADC250 with at 250 MHz sampling rate with a target goal of 100 ps timing resolution. The ASOC chip has a sampling rate from 2.4 to 3.2 GHz. We are evaluating the benefit of higher sampling rate on timing resolution in a high background environment.

Milestone	Objectives	Expected Completion Date	Status	Updated Date
E1	Acquire and setup ASOC evaluation board	April 15, 2020	Complete	
E2	Acquire data of scintillator	October 15, 2020	80% complete	May 1, 2021 +1 mo. conting.
E3	Complete analysis and determine achieved timing resolution with ASOC and compare to FADC resolution	February 15, 2021	Delayed	July 15, 2021 +1 mo. conting.

E1: Completed in the first quarter.

E2: On-going. E2 was delayed due to issue with not recording signal. After investigation and debugging with support from NALU it was concluded the board had an hardware issue and a spare was received in November which successfully recorded pulser and scintillator data. A test setup together with GEM VMM3 is being setup. This will be used to detect cosmics and correct the timing using position of the hits.

E3: On-going. Once E2 is completed, a measurement with a large background from a radioactive source will be carried out and timing resolution will be determined.

1.3 Budget / spending summary / procurement

No new expenses in this quarter. Main spending will happen in next quarter with building of the VMM prototype and test stands.

System	Cost ($)	Number	Total	Spent
VXS crate for DAQ modules	15,000	2	30,000	32,388
VTP - Module for triggering and data movement	10,000	2	20,000	17,050
SSP	6,500	1	6,500	0
TI - Trigger Interface	3,000	2	6,000	0
SD - Signal Distribution card	2,500	2	5,000	1,250
FADC trigger distribution card	2,000	2	4,000	4000
VME CPU	4,500	2	9,000	11,000
Trigger Supervisor	3,500	1	3,500	0
Hardware components for VMM readout test stand	25,000	1	25,000	6,775
APV25 GEM system	23,000	1	23,000	8,480
Cables/patch	400	160	64,000	8,000
Optical fibers	100	20	2,000	2,000
MAROC eval board	23,000	1	23,000	0
ASOC eval board	10,000	1	10,000	8000
Optical transceivers	50	32	1600	1600
Total M/S direct			210,600	102,487
Total request M/S			227,300	110,575
Workforce 2020	$130,000$	1.25	162,500	90,000
Workforce 2021	$133,900	1	133,900	203,518
Contract DG electronics	78,250	1	78,250	78,250

Table 1: Budget summary

	Budget ($)	Obligated ($)
Material	227,300	110,575
Personel	372,700	371,768
Total	600,000	474,255

Table 2: Budgeted and obligated funds summary (includes overhead)

2 High Rate Test of MaPMT Array and LAPPD Using a Telescopic Cherenkov Device

2.1 Summary

A detailed data analysis of electronics response and effective trigger configurations for the simple-sum MaPMT photo-detector readout from the parasitic beam testing in Hall-C has been completed. The results demonstrate that MaPMT meets the SoLID requirement under the expected high-rate environment. Comparisons of data with simulations show reasonable agreement. MaPMT bench tests using MAROC sum electronics are ongoing and are expected to be completed by the next quarterly report. Progress on those bench tests are presented below. Overall, the pre-R&D project is on schedule to successfully complete every goal as planned.

2.2 Project Milestones

Milestone	Objectives	Expected Completion Date	Status
1	Construction and delivery of Cherenkov tank to Jefferson Lab.	Early January 2020	Complete (Q1)
2	Cosmic testing and installation into experimental hall.	Mid February 2020	Complete (Q1)
3	Collection and analysis of low and high rate data with electronic summing-board.	End of Year 2020 (+2 Month Contingency)	Collection complete (Q2), Analysis completed (Q4).
4	Collection and analysis of high rate data with MAROC electronics.	End of Year 2020 (+4 Month Contingency)	Moved to bench and nearing completion.

2.3 Budget / spending summary / procurement

To date funds have been used to purchase all the materials to construct the Cherenkov prototype tank with pressure controls, all connectors and cables for reading out signals of 64 channels from MaPMTs or LAPPD, mirror, 16 MaPMTs, wavelength shifter coating, radiator gas, MAROC readout boards and their cabling. Funds have been used for the mechanical engineering design and machining as well as electrical engineering support, travel

	Budgeted	Q1 Expenses	Q2 Expenses	Q3 Expenses	Q4 Expenses
Material	$210,000	$124,736	$84,414	$3,311	($228.64)
Personnel	$240,000	$31,376	$27,411	$26,882	$47,915
Travel	0	0	0	$5,295	$3,509
Total	$450,000	$156,112	$111,825	$35,488	$51,195

Table 3: Budgeted and expenditures summary from both Temple and Duke for the Cherenkov prototype (includes overhead)

and transport of the prototype from Temple to Jefferson Lab, and the research personnel support for the approved activities at Duke and Temple.

2.4 Analysis and Simulation

In this quarter, several scenarios of trigger forming with the Cherenkov detector under a high-rate environment were studied. The analysis for MaPMT with low-rate and high-rate data has been finalized. The primary goal of the data analysis has been reached, showing that the MaPMT works well under total rates of over 8 MHz/PMT. Details about the rates determination, trigger scenarios, and the comparison with simulations are presented in the following subsections. In the future, we will further determine the LAPPD performance by combining the LAPPD bench test data.

2.4.1 Cherenkov Detector Rates with MaPMT

During the high-rate test, most of the data were taken with triggers from the calorimeter with a threshold slightly below the signal from minimum ionizing particles (MIP). As a reference, some of the data were also taken with a built-in pulser in the FADC250 module. These pulser runs were triggered with a fixed time interval, which is uncorrelated to the signals from any of the calorimeter or MaPMT channels. Simply counting the number of signals over the Cherenkov data-taking time would yield the total detector rates. During the pulser runs, the DAQ system is taking raw waveform data with a 256 ns window (64 samples with 1 sample per 4 ns). The pipeline data-taking mode and low rate of pulser triggers result in a 100% DAQ live time. Therefore, the total rates can be obtained from the pulser runs as

$$\text{rates} = \frac{\text{average counts of signals per window}}{\text{window size (256 ns)}}. \quad (1)$$

The signal counting was carried out with the peak-finding algorithm in the waveform analysis software. It finds the peaks that are statistically significant with a given threshold

on the peak height relative to the pedestal. Figure 8 shows an example of the peak finding for waveform data.

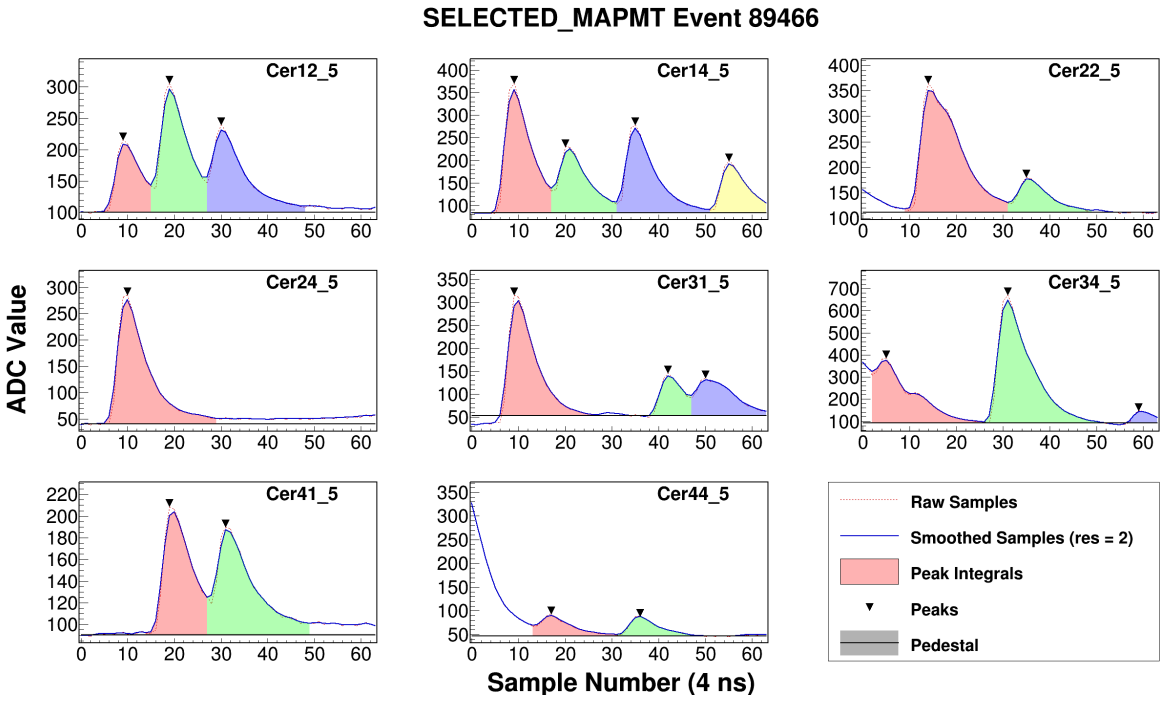

Figure 8: Waveform data for an event in a few selected MaPMT channels. The channels are named as CerXY with X the row and Y the column of the 4×4 MaPMT array (5 at the end represents the PMT sum channel, and 1-4 denote the quadrant channels). Raw samples are shown as a red dashed line and smoothed samples (rolling weighted average) are shown as a blue line. The two lines are mostly identical with a smoothing window of size 2. Identified peaks are colored and the peak positions are marked with inverted triangles. Pedestal was determined event-by-event, and is shown as a black line with a grey shade representing its error. The peak-finding algorithm uses a threshold of 20 ADC channel above the pedestal.

Among the pulser trigger runs, run 308 was taken following a production run 307, with the same beam current and target. The rates extracted from run 308 is shown in Figure 9, with a peak finding threshold of at the 20 ADC channel above the pedestal, which is about 1/4 of single photo-electron (SPE) amplitude. The threshold was set relative low to account for all the possible backgrounds. For all MaPMTs, the fluctuation of pedestals is a distribution with $\sigma < 5$ ADC channels, so a cut at the 20 ADC channel is over 4σ of the pedestal distribution. We have also varied the threshold with 0.25 SPE (40 ADC channel) and 1.0 SPE (80 ADC channel), and summarized the results in Table 4. The pulser run analysis shows the maximum detector rate is 8.2 MHz/PMT, with an average value of 7.1 MHz/PMT.

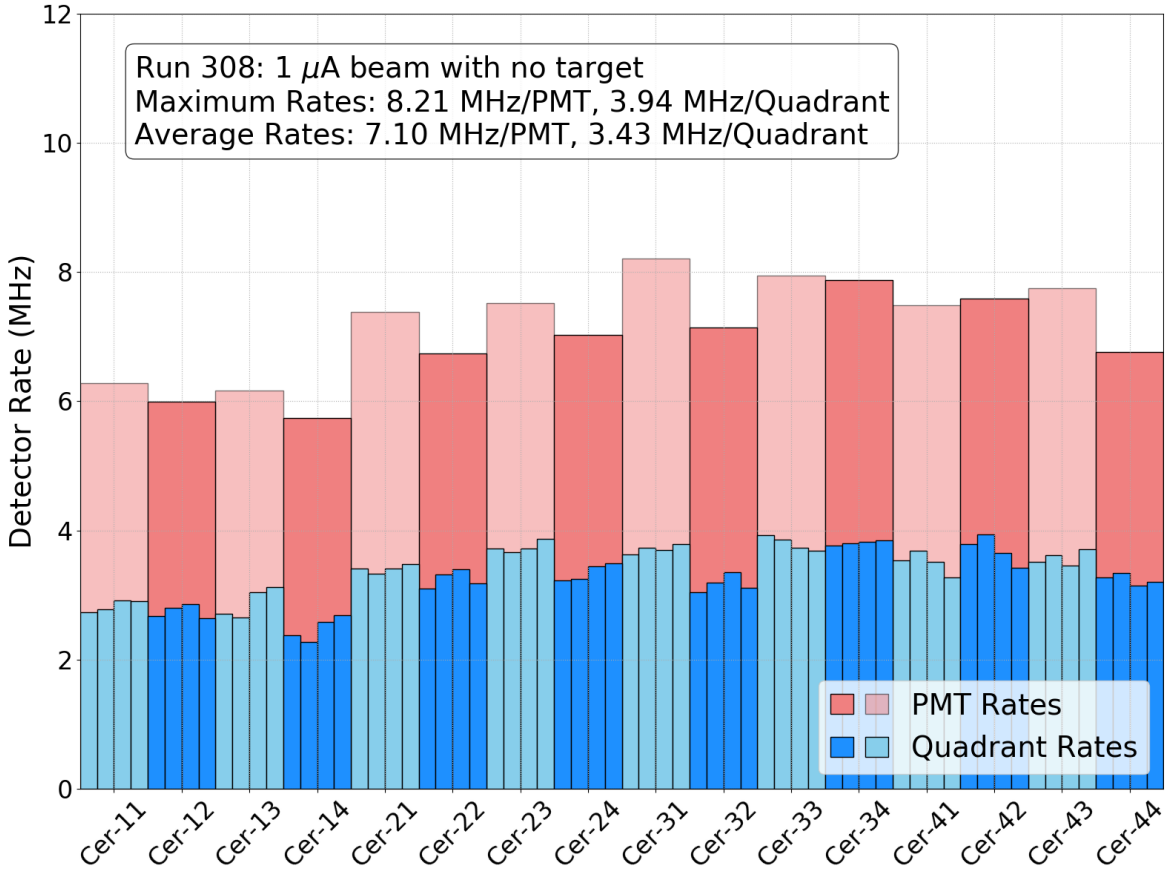

Figure 9: Cherenkov detector rates per PMT or quadrant channel from run 308. The rates per PMT are shown as red bars, and the rates per quadrant are shown as blue bars. The peak-finding algorithm used a threshold of 20 ADC channel, which is about 1/4 of the single photo-electron signal. The MaPMT channels are named as Cer-XY in accordance with the front view of the MaPMT array, with X the row and Y the column.

Configuration	Rates per PMT (MHz)		Rates per Quadrant (MHz)	
	Maximum	Average	Maximum	Average
Data Npe $>$ 0.25	8.21	7.10	3.94	3.43
Data Npe $>$ 0.50	7.88	6.83	3.65	3.10
Data Npe $>$ 1.00	6.95	5.87	2.70	1.95
Simulation Npe $>$ 0	6.4	6.0	3.0	2.8
Simulation Npe $>$ 1	4.5	4.2	1.5	1.4

Table 4: Cherenkov detector rates with different values of threshold and simulation results

We simulated the TCD high-rate test condition in Geant4 as shown in Figure 10. During the "no target" run 307 and 308, 1 uA of 10.4 GeV electron beam passing through the

upstream Be and Al windows, 76 cm long nitrogen gas in the target area, then downstream Al and Be windows in turn with a total luminosity of about $0.9 \times 10^{36} cm^{-2} s^{-1}$. The TCD was at the nominal position of 3.5 degree polar angle on the right side of the beam, 0 degree alignment angle aiming at the target center, and 12 m away. Its opening angle ∼1.5 degree is large enough to cover the entire 76 cm target area. At such a small polar angle, beam electrons can produce a lot of secondary particles from the downstream beamline. Figure 11 shows the vertex and momentum of mother particles (dominantly electrons and positrons) which produce Cherenkov lights detected by the MaPMT assembly. The contribution from the beamline windows, nitrogen gas, and downstream beamline walls can be seen clearly. The mother particles have momentum range from 16 MeV/c at the CO_2 gas threshold to a couple GeV/c and are mostly created by electron ionization and gamma conversion. During the runs, the HallC SHMS is at 11 degree left to the beamline and the dipole field from its Horizontal Bender (HB) magnet is set for a central momentum value of -7.5 GeV/c. The HB fringe field was implemented in the simulation because it can reach a few hundred Gauss and thus bend those low energy mother particles.

We tried to simulate the beam test condition as closely as possible. Nevertheless, as a parasitic test, it has many uncertainties. For example, the TCD polar angle and alignment angle has an error of ∼0.5 degree, and it can change Cherenkov detector rate by ±15%. Another factor is beam stability. As the Hall C beam control is optimized for high beam currents like 30 uA, a 1 uA beam could be a couple mm off the beam path and have much large beam profile than the 4.5 mm diameter controlled by the raster. This could increase the rate as much as 15%. Finally, the uncertainty in HB fringe field can affect the rate up to 20%. Overall the low current, small angle and long distance configuration made it difficult to control various aspects of the setting to very good precision. Therefore one needs to take these into consideration when comparing simulated results to the data. We also tested different versions of Geant4 and observed 10% differences in rate.

The rates from simulation with Geant4.10.06.p02 released in May 2020 and the nominal running conditions are listed in Table 4. We chose Npe > 0 or 1 to compare to the data with similar cuts. In general, the agreement between the simulation and the data is about 50-80% for all PMT and quadrant results, which is encouraging given the aforementioned systematic issues. The maximum rate of 8.2 MHz/PMT from the data and the 6.4 MHz/PMT from the simulation, agree to $\sim$ 80%, which is quite remarkable given the parasitic nature of the beam test making it difficult to control various systematic aspects of the test. They both exceed the maximum SoLID Cherenkov detector rate of 4 MHz/PMT estimated using the same simulation program and Npe > 0 condition.

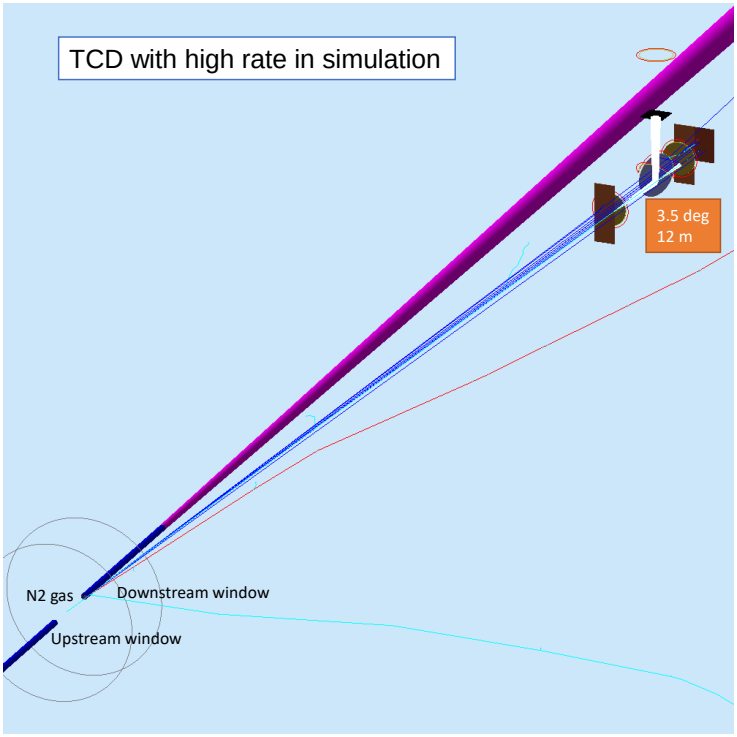

Figure 10: TCD setup at the small angle for the high-rate test. One electron (cyan) is from the target center producing Cherenkov light (white) in TCD. There are secondary gamma rays (blue) and positrons (red) produced along the way according to Geant4 physics.

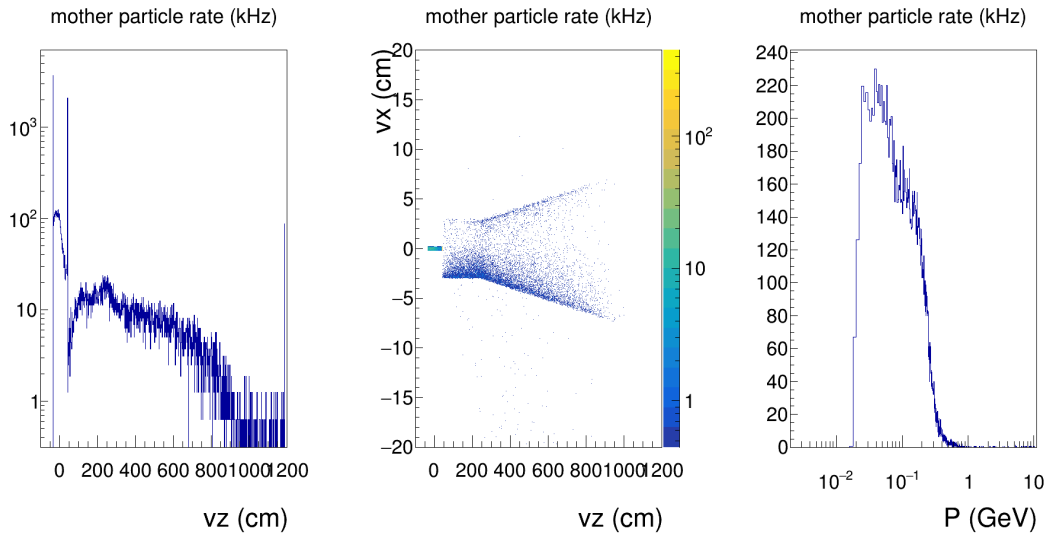

Figure 11: The vertex and momentum of mother particles (electrons and positrons) which produce Cherenkov light in TCD. Their momentum ranges from 16 MeV/c at the CO_2 gas threshold to a couple GeV/c. TCD has a wide acceptance of mother particles from the entire target area and downstream beamline components.

2.4.2 Cherenkov Trigger Forming and Efficiency

The pulser run 308 shows the prototype detector was operating with a maximum rate of 8.2 MHz/PMT. The production run 307 was taken just prior to run 308, with the same beam current and target. In this subsection, we present the study of Cherenkov trigger with run 307 data, which demonstrates that the coincidence triggers could reject most of the backgrounds under the high-rate environment.

The raw waveform data were analyzed following the same procedure described in the previous quarterly report. A 20-ns-wide timing cut was performed on the MaPMT signal timings relative to the triggered calorimeter channel to select the signals. In this study, we also selected the events triggered by the central calorimeter blocks, as shown in Figure 12. This geometrical cut helps select the events with a full acceptance of the Cherenkov light cones on the 4×4 MaPMT array.

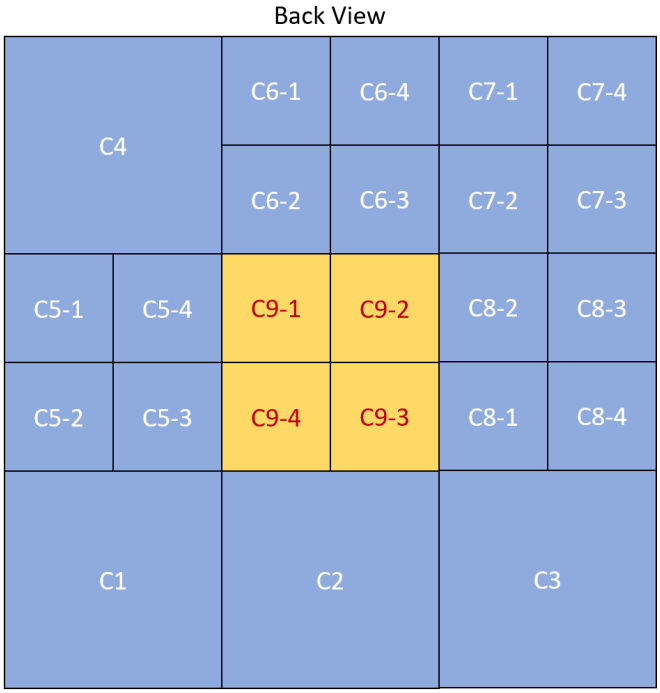

Figure 12: Layout of the calorimeter blocks. The blocks that pass the geometrical cut are colored yellow.

Figure 13 shows the 2D distribution of the number of fired MaPMTs (NPMT) and the number of photo-electron (Npe) from the signal sum for both data and simulation. The selected events are overwhelmed by random backgrounds with low Npe and NPMT. Therefore, most of the backgrounds can be rejected by simply requiring a coincidence between 2 PMT channels, as shown in the bottom panel of Figure 13. With a coincidence of 2 PMT channels, we can achieve a signal to background ratio of about 2:1, without any significant

loss of signals.

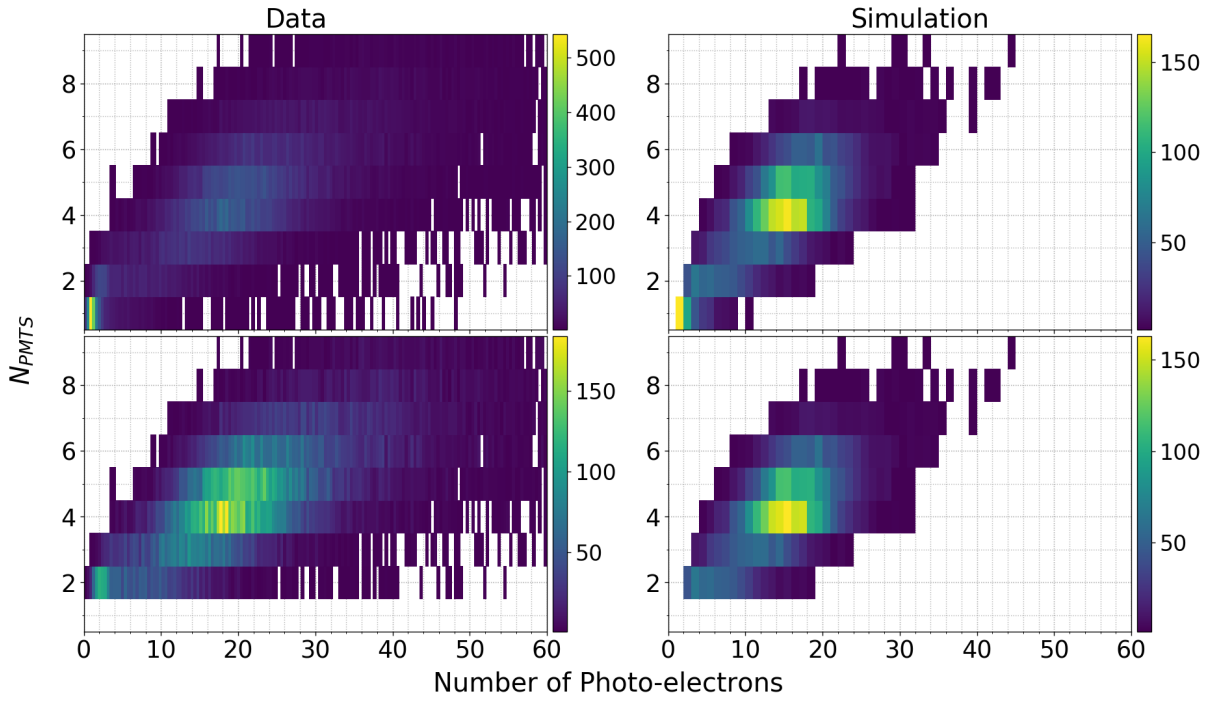

Figure 13: number of fired PMT channels (N_{PMT}) vs. number of photo-electrons (N_{pe}) from the selected events for data (left) and simulation (right). The top panel shows the distribution without any cut, while the bottom panel shows the same distribution with $N_{PMT} \geq 2$. The Cherenkov signal is revealed with the coincidence cut, centered around $N_{PMT} = 4$ and $N_{pe} = 18$.

A similar analysis was performed with the PMT quadrant signals, and the results are shown in Figure 14. It was found that a coincidence of 3 quadrant channels would suffice to raise the signal to background ratio to about 3:1, without any noticeable loss of signals.

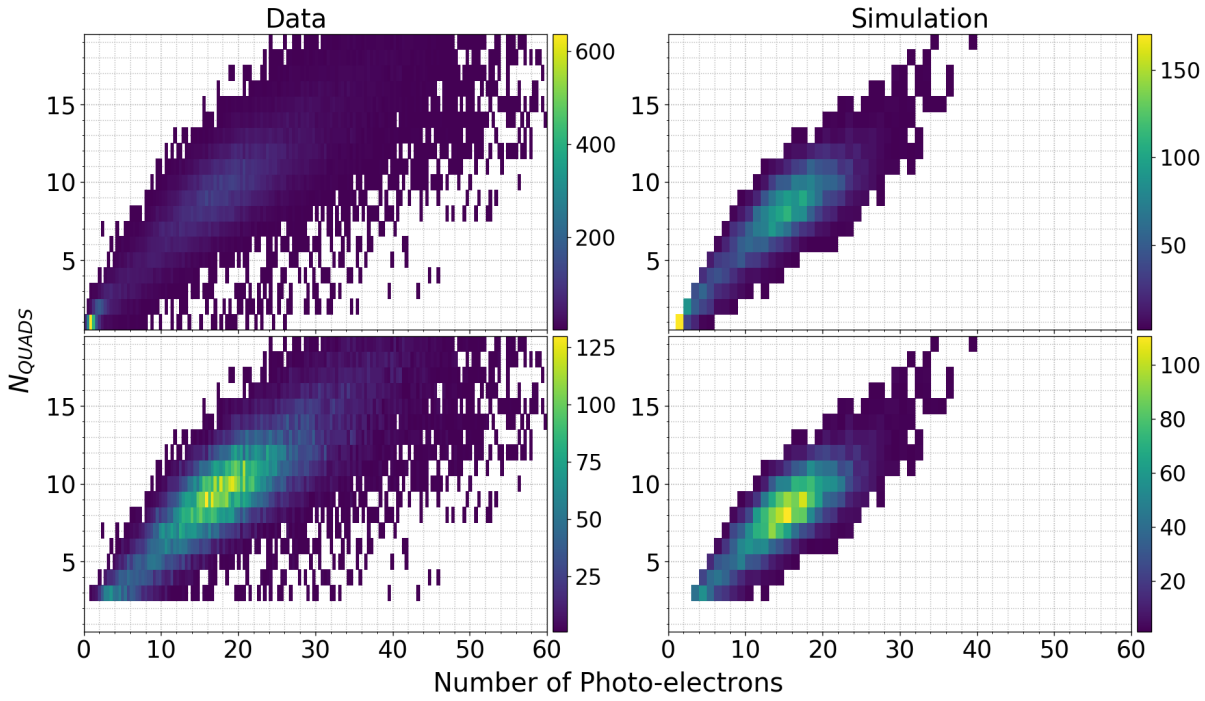

Figure 14: number of fired PMT quadrant channels (N_{QUADS}) vs. number of photo-electrons (N_{pe}) from the selected events for data (left) and simulation (right). The top panel shows the distribution without any cut, while the bottom panel shows the same distribution with $N_{QUADS} \geq 3$. The Cherenkov signal is revealed with the coincidence cut, centered around $N_{QUADS} = 9$ and $N_{pe} = 18$.

In conclusion, the data analysis of the production run 307 and the pulser run 308 demonstrates that the prototype detector could work well under a high rate of 8.2 MHz/PMT. The majority of the backgrounds can be simply rejected by forming a coincidence between 2 PMT or 3 quadrant channels. This coincidence cut, as shown in the bottom panels of Figure 13 and 14, is well below the Cherenkov signals, hence results in a little loss of the signals.

2.5 MaPMT with MAROC sum readout bench test

In this quarter, we tested the performance of the MaPMT and front-end electronics up to the expected maximum SoLID rates, 200 kHz/pixel for pixel readout and 4 MHz/PMT for sum readout, using LEDs and a laser as light sources. The schematic layout for the bench test is shown in Figure 15. Pulsed laser (470 nm) was used as signal and LED (275 nm) operated with DC voltage was used to mimic the background. The amount of light from the LED was controlled by changing the applied DC voltage. Laser lights are diffused to cover the entire MaPMT surface and filtered to allow three different laser light intensities: strong, medium, and weak laser light. Light from LED and laser was collected by the WLS coated Hamamatsu H12700-03 MaPMT (SN HA0037). MaPMT was read out by MAROC

sum board which gave two independent pieces of information: TDC signal from 64 pixels and 5 FADC sum signals including 4 quads of 16 pixels each and 1 sum of 64 pixels. An independent pulse generator (clock) was used as triggers for both DAQ (JLab CODA system) and the pulsed laser. Along with CODA data, we also have the scaler data for all 64 pixels and all sum signals.

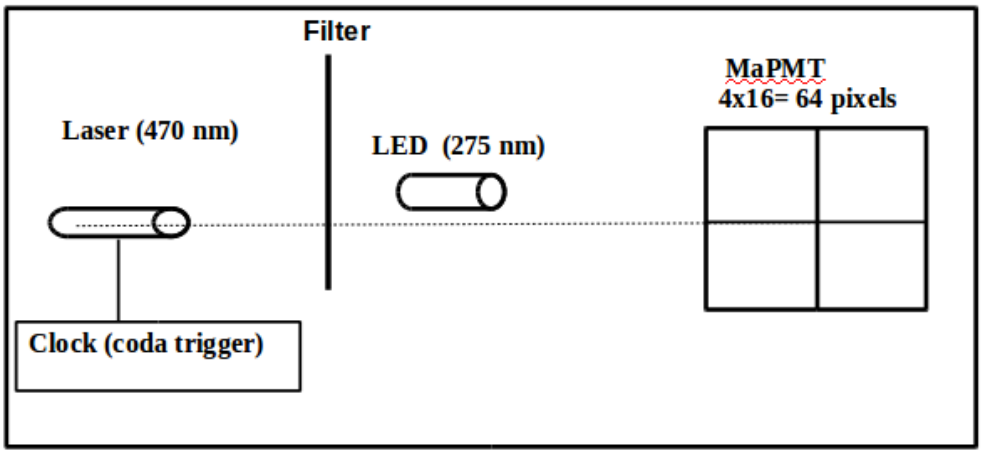

Figure 15: Schematic layout of bench test set up. The entire setup was placed inside the black box to minimize the background.

Figure 16 shows the FADC waveform for beam test (left) and bench test (right). It demonstrates using LED as random background and laser as a signal, we produced the condition similar to the beam test.

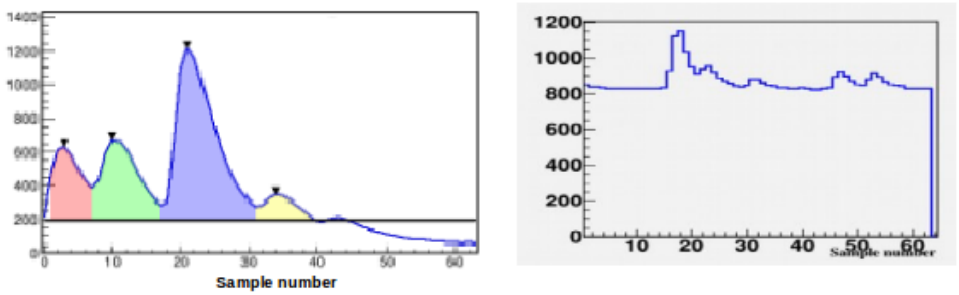

Figure 16: Left: FADC waveform for beam test data. Right: FADC waveform for bench test with LED and laser, which were used to mimic the condition similar in beam test.

The average pixel rate from pixel scaler rises linearly with the output laser repetition frequency for three different laser light intensities as expected, see Figure 17. With strong laser light and LED operated at DC voltage of 2.15 V, we achieved the average pixel rate $\sim$ 550 kHz/pixel, a factor of 2.8 times larger than the max pixel rate expected in the SoLID.

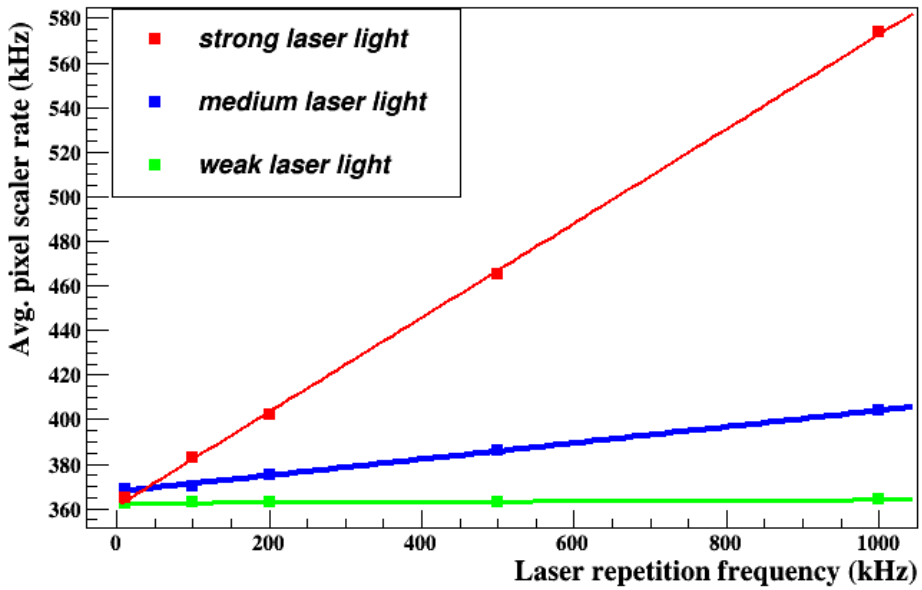

Figure 17: The linear relation between the output laser repetition frequency with average pixel rate. With LED at 2.15 V and laser operating at 1 MHz, we achieved the pixel rate up to ∼550 kHZ/pixel which is more than twice larger than as expected in the SoLID.

In the case of TDC, the single event may result in multiple pixel hits but the FADC sums as a single event. The two scalers: pixel scaler and sum scaler rate can be related using Equation 2.

$$\text{Sum scaler rate} = \frac{\text{Average pixel scaler rate} \times 64}{\text{Average pixel occupancy}} \tag{2}$$

where average pixel scaler rate is an average hit of 64 pixels and the average pixel occupancy is an average number of pixel hits for an event. Figure 18 shows the agreement between rates from the sum scaler and pixel scaler for LED operating at different DC voltage is within 3%. With LED operating in DC, we achieved the background rate ∼ 6 MHz/PMT, larger than expected in SoLID.

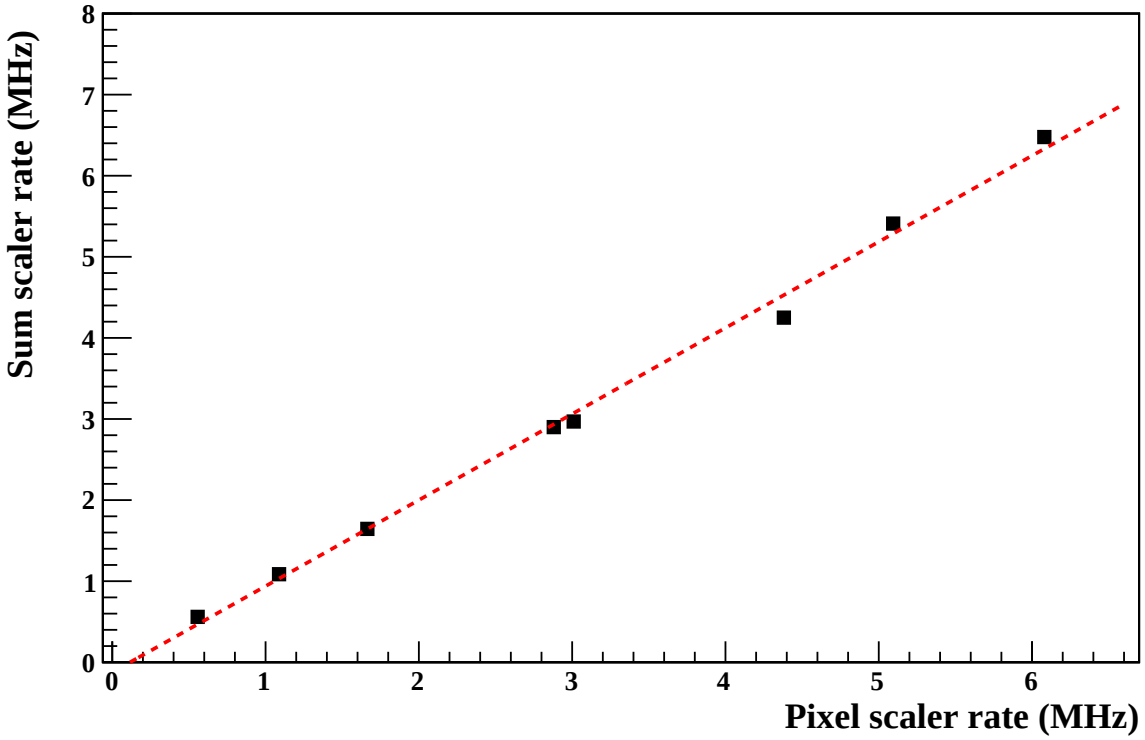

Figure 18: Comparison between the sum and pixel scaler rates. The agreement between the two scaler rates are within 3% for rates similar to that expected in SoLID.

One of the goals of this test was to check the performance of MAROC electronics. The linear correlation between pixel signals readout by MAROC TDCs and sum signals readout by flash ADCs has been established for the rates similar to the SoLID running condition. Figure 19 shows the linear correlation between TDC and FADC signal (left: sum signal and right: quad signal) for the sum rate ∼4 MHz/PMT and pixel rate ∼260 kHz/pixel. This demonstrates that summing electronics work as expected to collect the charge from pixels.

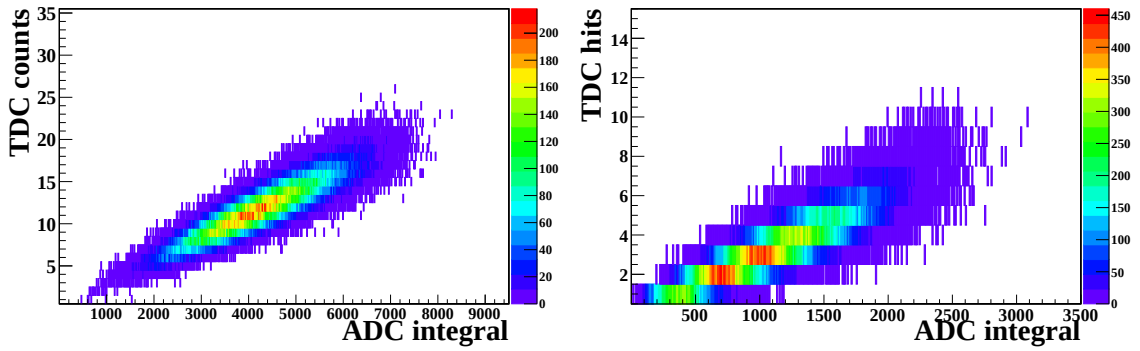

Figure 19: Left: TDC counts VS ADC total sum signal. Right: TDC counts vs ADC one quadrant sum signal. The linear correlation between pixel signals read-out by MAROC TDCs and sum signals read-out by flash ADCs is observed from the MaPMT with MAROC sum readout tested with LED.

The second goal of the test is to understand how well we can separate the signal from the background at a rate similar to the SoLID running condition. Figure 20 shows the FADC waveform for sum signal with both laser and LED on. The laser signal arrives at a fixed time window as shown by two vertical red lines whereas the background from LED is random in time. With the appropriate timing cut, the signal can be separated from the background unless the background and signal both arrive at the same time interval.

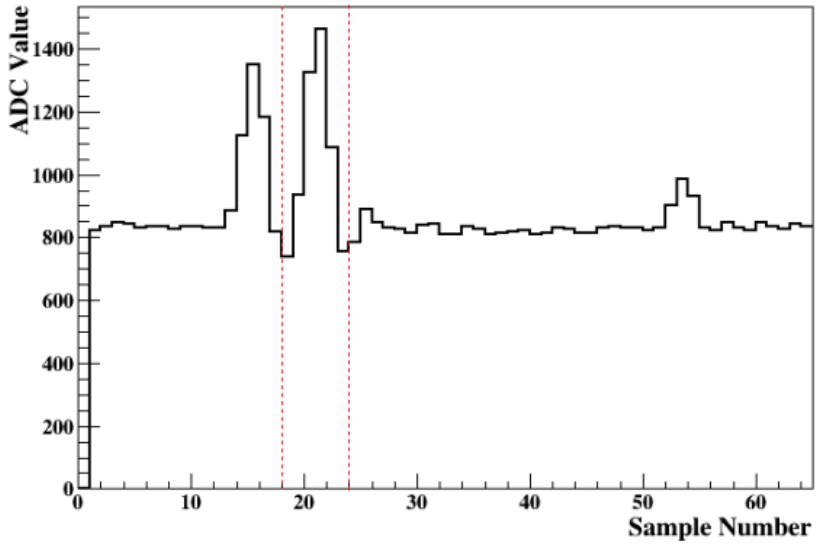

Figure 20: FADC waveform for sum signal. The laser signal arrives at fixed FADC time window represented by vertical lines while the background from LED are random in time.

Figure 21 shows the comparison of ADC integral between the runs: both laser and LED on (signal and background) after applying the timing cut and run with laser on but LED

off (signal only). The running condition is equivalent to the sum signal rate $\sim$ 4MHz/PMT. The agreement of ADC integral between the runs with and without LED after the FADC time cut demonstrates that with appropriate FADC timing cut we can separate the signal from background very well to a rate as high as expected in the SoLID.

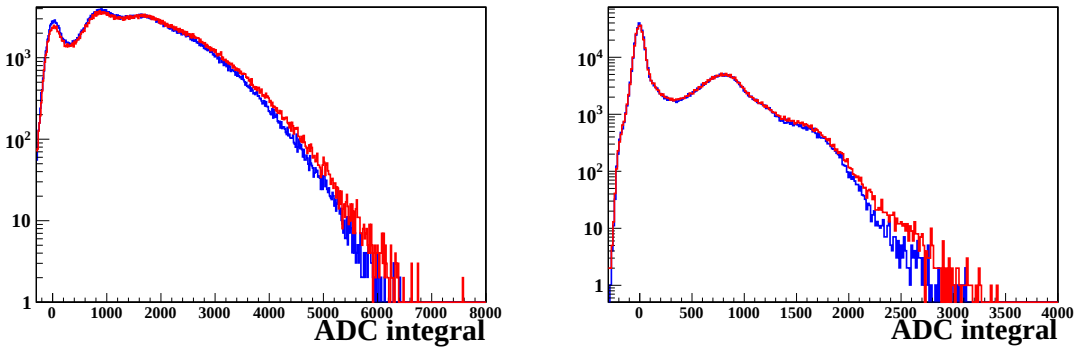

Figure 21: Background subtraction with FADC time cut. Left: FADC sum signal. Right: FADC Quad signal. The red histogram is the ADC integral after the FADC timing cut for a run with both laser (weak laser) and LED on. The blue histogram is for a run with a laser (weak laser) on and LED off.

Currently, we are performing a cosmic test using lucite as a Cherenkov radiator. The main goals of this test is to examine how the entire system behaves with real Cherenkov signals and to understand how well we can separate the random background based on Cherenkov ring. As the cosmic ray passes through the lucite, refractive index (μ) 1.50, the Cherenkov light is emitted. The emitted Cherenkov light can be collected with a MaPMT array. In addition, we are also planning to take cosmic data in presence of random background from the LED to study the background subtraction. We are planning to finish the cosmic ray test by the end of April, 2021.